

BENDING OF CURVED COMPOSITE BEAM WITH INTERLAYER SLIP

Attila Baksa 

associate professor, Institute of Applied Mechanics
3515 Miskolc-Egyetemváros, e-mail: attila.baksa@uni-miskolc.hu

István Ecsedi 

professor emeritus, Institute of Applied Mechanics
3515 Miskolc-Egyetemváros, e-mail: istvan.ecsedi@uni-miskolc.hu

Abstract

Elastic two-layer curved composite beam with partial shear interaction is considered. It is assumed that each curved layer separately follows the Euler-Bernoulli hypothesis and the load slip relation for the flexible shear connection is a linear relationship. The curved composite beam is subjected to uniform bending. The paper presents solutions for stresses, radial displacement, and slip.

The end cross sections of the layered curved beam are loaded by zero moment force couples, as a result of which each cross section of the beam is loaded by zero moment force couple resultant.

Keywords: composite, curved beam, weak shear connection, bending, slip

1. Introduction

The problem of layered beam with straight centreline and with deformable shear connection has been studied for a long time. The first mathematical theories of this type of composite beams were developed by (Granholm, 1949), (Pleskov, 1952), (Stüssi, 1947) and (Newmark et al., 1951). Today the analytical and numerical solutions and refine of the theory of beams with flexible shear connections are presented by several authors such as (Girhammar and Gopu, 1993), (Planic et al., 2008), (Girhammar and Pan, 2007) and (Goodman and Popov, 1968, 1969). Authors studied the two layered curved beam with partial shear interaction (Ecsedi and Lengyel, 2015). They considered static problems (Ecsedi and Dluhi, 2005). There exist many other works on this topic, it is not the aim of this paper to give a complete list on the layered beams with flexible shear connections. In this paper we consider two-layer composite curved beams with deformable shear connector. The curved beam is subjected to bending moments applied them at the its end cross-sections. The considered two-layer curved beam configuration is shown in *Figure 1*. In the cylindrical coordinate system $Or\varphi z$ the curved layer i ($i = 1,2$) occupies the space domain B_i ($i = 1,2$)

$$B_i = \{(r, \varphi, z) | (r, z) \in A_i, 0 \leq \varphi \leq \pi\} \quad (1)$$

where A_i is the cross section of beam component i ($i = 1,2$) *Figure 1*. The common boundary of B_1 and B_2 is denoted by ∂B_{12}

Application of the strain-displacement relationships of the linearized theory of elasticity gives (Sokolnikoff, 1956)

$$\varepsilon_r = \varepsilon_z = \gamma_{r\varphi} = \gamma_{rz} = \gamma_{\varphi z} = 0. \quad (r, \varphi, z) \in B_1 \cup B_2, \quad (6)$$

$$\varepsilon_\varphi = \frac{1}{r} \left(\frac{d^2 U}{d\varphi^2} + U \right) + \frac{d\phi_i}{d\varphi}, \quad (r, \varphi, z) \in B_i \quad (i = 1, 2). \quad (7)$$

In *equations (6) and (7)* ε_r , ε_φ and ε_z are the normal strains and $\gamma_{r\varphi}$, γ_{rz} , and $\gamma_{\varphi z}$ are the shearing strains. The strains given by *equation (7)* satisfy the requirements of the Euler–Bernoulli beam theory, only the one normal strain component ε_φ is different from zero and all the shearing strains vanish. From the definition of the interlayer slip $s = s(\varphi)$ it follows that (*Figure 1*)

$$s(\varphi) = c(\phi_1(\varphi) - \phi_2(\varphi)) \quad (8)$$

Denote $\tilde{T} = \tilde{T}(\varphi)$ the interlayer shear force acting on unit area of the common boundary surface of B_1 and B_2 , which is $c t d\varphi$. The value of the interlayer shear force on this surface element is

$$T(\varphi)d\varphi = \tilde{T}ct d\varphi = kc^2t(\phi_1(\varphi) - \phi_2(\varphi))d\varphi \quad (9)$$

that is

$$T(\varphi) = kc^2t(\phi_1(\varphi) - \phi_2(\varphi)). \quad (10)$$

Here we assume that

$$\tilde{T}(\varphi) = ks(\varphi) \quad (11)$$

and we note that the unit of slip modulus k is [force/length³]. According to paper (Ecsedi and Dluhi, 2005) we define the stress resultants normal force N , shearing force S and stress couple resultants M_i ($i = 1, 2$) such as

$$N_i = \int_{A_i} \sigma_\varphi dA, \quad S_i = \int_{A_i} \tau_{r\varphi} dA, \quad M_i = \int_{A_i} r\sigma_\varphi dA, \quad (i = 1, 2). \quad (12)$$

The virtual work of the section forces and moment on a kinematically admissible displacement field

$$\tilde{u} = \tilde{U}(\varphi), \quad \tilde{w} = 0, \quad \tilde{v} = r\tilde{\phi}_i + \frac{d\tilde{U}}{d\varphi}, \quad (i = 1, 2) \quad (13)$$

can be computed as

$$\begin{aligned} \tilde{W} &= \int_A \sigma_\varphi \tilde{v} dA + \int_A \tau_{r\varphi} \tilde{u} dA = M_1 \tilde{\phi}_1 + M_2 \tilde{\phi}_2 + N \frac{d\tilde{U}}{d\varphi} + S \tilde{U}, \\ N &= N_1 + N_2, \quad S = S_1 + S_2 \end{aligned} \quad (14)$$

From *equation (14)* we obtain the possible combinations of the boundary conditions at the end cross sections

- $S = S_1 + S_2$ or U may be prescribed.
- $N = N_1 + N_2$ or $V(\varphi) = dU/d\varphi$ may be prescribed.
- M_1 or ϕ_1 may be prescribed.
- M_2 or ϕ_2 may be prescribed.

Application of Hooke's law yields the formula of normal stress σ_φ

$$\sigma_\varphi = E_i \left[\frac{1}{r} \left(\frac{d^2 U}{d\varphi^2} + U \right) + \frac{d\phi_i}{d\varphi} \right] \quad (r, \varphi, z) \in B_i \quad (i = 1, 2), \quad (15)$$

where E_i is the modulus of elasticity for curved layer i ($i = 1, 2$). Combination of *equation (12)* and *(15)* gives

$$N_i = \frac{A_i E_i}{R_i} \left(\frac{d^2 U}{d\varphi^2} + U \right) + A_i E_i \frac{d\phi_i}{d\varphi}, \quad (i = 1, 2). \quad (16)$$

$$M_i = A_i E_i \left(\frac{d^2 U}{d\varphi^2} + U \right) + r_i A_i E_i \frac{d\phi_i}{d\varphi}, \quad (i = 1, 2). \quad (17)$$

Here,

$$\frac{1}{R_i} = \frac{1}{A_i} \int_{A_i} \frac{dA}{r}, \quad (i = 1, 2), \quad (18)$$

$$r_i = \frac{1}{A_i} \int_{A_i} r dA, \quad \overline{OC}_i = r_i, \quad (i = 1, 2). \quad (19)$$

It is evident in the present problem, shown in *figure 1*,

$$N = \frac{A E_0}{R} W + A_1 E_1 \frac{d\phi_1}{d\varphi} + A_2 E_2 \frac{d\phi_2}{d\varphi} = 0 \quad (20)$$

$$M = M_1 + M_2 = A E_0 W + r_1 A_1 E_1 \frac{d\phi_1}{d\varphi} + r_2 A_2 E_2 \frac{d\phi_2}{d\varphi} = M_0 = \text{const.} \quad (21)$$

Here, E_0 and R are defined as

$$E_0 = \frac{1}{A} (A_1 E_1 + A_2 E_2), \quad A = A_1 + A_2, \quad (22)$$

$$\frac{A E_0}{R} = \frac{A_1 E_1}{R_1} + \frac{A_2 E_2}{R_2}, \quad (23)$$

and

$$W(\varphi) = \frac{d^2 U}{d\varphi^2} + U(\varphi), \quad (24)$$

and the total bending moment is denoted by M_0 . According to *equation (10)* of paper (Ecsedi and Dluhi, 2005) we can write

$$S = -\frac{dN}{d\varphi} = -\left(\frac{A E_0}{R} \frac{dW}{d\varphi} + A_1 E_1 \frac{d^2 \phi_1}{d\varphi^2} + A_2 E_2 \frac{d^2 \phi_2}{d\varphi^2} \right) = 0 \quad (25)$$

Moment equilibrium equation for curved beam component 1 can be formulated as

$$\frac{dM_1}{d\varphi} + m_1(\varphi) = 0, \quad (26)$$

where the source of $m_1 = m_1(\varphi)$ is the interlayer shear force (*Figure 2*), that is

$$m_1(\varphi) = -cT(\varphi) = -kc^3 t [\phi_1(\varphi) - \phi_2(\varphi)]. \quad (27)$$

Substitution of *equation (27)* into *equation (26)* gives

$$A_1 E_1 \frac{dW}{d\varphi} + r_1 A_1 E_1 \frac{d^2 \phi_1}{d\varphi^2} - kc^3 t [\phi_1 - \phi_2] = 0. \quad (28)$$

Here, we note *equation (26)* follows from *equation (12)* of paper (Ecsedi and Dluhi, 2005).

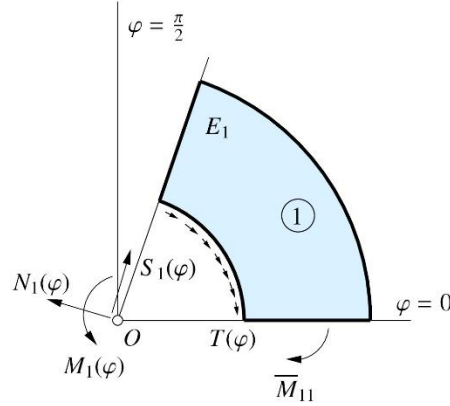


Figure 2. Stress and stress couple resultants and interlayer shear force on beam component 1

From *equations (20)* and *(21)* it follows that

$$R \frac{A_1 E_1}{A E_0} \frac{d\phi_1}{d\varphi} + R \frac{A_2 E_2}{A E_0} \frac{d\phi_2}{d\varphi} = -W, \quad (29)$$

$$r_1 \frac{A_1 E_1}{A E_0} \frac{d\phi_1}{d\varphi} + r_2 \frac{A_2 E_2}{A E_0} \frac{d\phi_2}{d\varphi} = -W + \frac{M_0}{A E_0}. \quad (30)$$

Solution of system of *equations (29)* and *(30)* for $\frac{d\phi_1}{d\varphi}$ and $\frac{d\phi_2}{d\varphi}$ is as follows

$$\frac{d\phi_1}{d\varphi} = \frac{E_0 A}{E_1 A_1} \frac{R - r_2}{r_2 - r_1} \frac{W}{R} - \frac{M_0}{E_1 A_1 (r_2 - r_1)}, \quad (31)$$

$$\frac{d\phi_2}{d\varphi} = \frac{E_0 A}{E_2 A_2} \frac{r_1 - R}{r_2 - r_1} \frac{W}{R} + \frac{M_0}{E_2 A_2 (r_2 - r_1)}. \quad (32)$$

Differentiation of *equation (28)* with respect to φ gives

$$\frac{d^2 W}{d\varphi^2} + r_1 \frac{d^3 \phi_1}{d\varphi^3} - \frac{kc^3 t}{A_1 E_1} \left(\frac{d\phi_1}{d\varphi} - \frac{d\phi_2}{d\varphi} \right) = 0. \quad (33)$$

Substitution of *equations (31)* and *(32)* into *equation (33)* leads to a second order differential equation for $W = W(\varphi)$

$$\frac{d^2 W}{d\varphi^2} \left(1 + \frac{E_0 A}{E_1 A_1} \frac{R - r_2}{r_2 - r_1} \frac{r_1}{R} \right) - \frac{kc^3 t}{A_2 E_2} \left(\frac{E_0 A}{E_1 A_1} \right)^2 \frac{R - r_3}{r_2 - r_1} \frac{W}{R} + \frac{kc^3 t}{(E_1 A_1)^2} \frac{E_0 A}{E_2 A_2} \frac{M_0}{r_2 - r_1} = 0. \quad (34)$$

In *equation (34)* r_3 is defined as

$$r_3 = \frac{r_1 A_1 E_1 + r_2 A_2 E_2}{A_1 E_1 + A_2 E_2}. \quad (35)$$

3. Determination of $W = W(\varphi)$

The general solution of differential equation (34) can be represented as

$$W(\varphi) = K_1 \sinh(\Omega\varphi) + K_2 \cosh(\Omega\varphi) + \frac{M_0 R}{E_0 A (R - r_3)}. \quad (36)$$

where $M_0 = \bar{M}_{11} + \bar{M}_{21} = \bar{M}_{12} + \bar{M}_{22}$, K_1 and K_2 are constants of the integration and

$$\Omega = \left[\frac{kc^3 t \left(\frac{E_0 A}{A_2 E_2} \frac{E_1 A_1}{E_1 A_1} \right)^2 \frac{R - r_3}{(r_2 - r_1) R}}{1 + \frac{E_0 A}{E_1 A_1} \frac{R - r_2}{r_2 - r_1} \frac{r_1}{R}} \right]^{\frac{1}{2}}, \quad (37)$$

K_1 and K_2 are computed from the stress boundary conditions (see Figure 1)

$$M_1(-\alpha) = \bar{M}_{11}, \quad M_2(-\alpha) = \bar{M}_{21} = M_0 - \bar{M}_{11}, \quad (38)$$

$$M_1(\alpha) = \bar{M}_{12}, \quad M_2(\alpha) = \bar{M}_{22} = M_0 - \bar{M}_{12}. \quad (39)$$

Application of equations (17), (31), (38) and (39) gives

$$W(-\alpha) = \frac{r_2 \bar{M}_{11} + r_1 \bar{M}_{21}}{E_1 A_1 (r_2 - r_1) \left(1 + \frac{r_1}{R} \frac{R - r_2}{r_2 - r_1} \frac{E_0 A}{E_1 A_1} \right)}, \quad (40)$$

$$W(\alpha) = \frac{r_2 \bar{M}_{12} + r_1 \bar{M}_{22}}{E_1 A_1 (r_2 - r_1) \left(1 + \frac{r_1}{R} \frac{R - r_2}{r_2 - r_1} \frac{E_0 A}{E_1 A_1} \right)}. \quad (41)$$

Here we note, the boundary condition (38)₁ and (38)₂ give the same equations for $W(-\alpha_1)$ and similar statement is valid for the boundary conditions (39)₁ and (39)₂, they give the same results for $W(\alpha_1)$.

From equations (40) and (41), assuming that α_1 is zero, we obtain

$$K_2 = \frac{r_2 \bar{M}_{11} + r_1 \bar{M}_{21}}{E_1 A_1 (r_2 - r_1) \left(1 + \frac{r_1}{R} \frac{R - r_2}{r_2 - r_1} \frac{E_0 A}{E_1 A_1} \right)} - \frac{(\bar{M}_{11} + \bar{M}_{21}) R}{E_0 A (R - r_3)}, \quad (42)$$

$$K_1 = \frac{r_2 \bar{M}_{11} + r_1 \bar{M}_{21}}{E_1 A_1 (r_2 - r_1) \left(1 + \frac{r_1}{R} \frac{R - r_2}{r_2 - r_1} \frac{E_0 A}{E_1 A_1} \right) \sinh(\Omega \alpha_2)} - \frac{(\bar{M}_{12} + \bar{M}_{22}) R}{E_0 A (R - r_3) \sinh(\Omega \alpha_2)} - K_2 \frac{\cosh(\Omega \alpha_2)}{\sinh(\Omega \alpha_2)}. \quad (43)$$

4. Determination of stress and radial displacement

The circumferential normal stress can be computed by the application of equation (15)

$$\sigma_\varphi(r, \varphi) = E_i \left[\frac{W}{r} + \frac{d\phi_i}{d\varphi} \right], \quad (r, \varphi, z) \in B_i \quad (i = 1, 2), \quad (44)$$

where $W = W(\varphi)$ and $d\phi_i/d\varphi$ are given by equations (36), (31) and (32).

Assuming that the non-zero stresses are $\sigma_\varphi = \sigma_\varphi(r, \varphi)$, $\tau_{r\varphi} = \tau_{r\varphi}(r, \varphi)$ and $\sigma_r = \sigma_r(r, \varphi)$ we can derive the following equilibrium equations

$$\frac{\partial}{\partial r} (rt(r)\sigma_r) - t(r)\sigma_\varphi + t(r) \frac{\partial \tau_{r\varphi}}{\partial \varphi} = 0, \quad (45)$$

$$\frac{\partial}{\partial r} (r^2 t(r)\tau_{r\varphi}) + rt(r) \frac{\partial \sigma_\varphi}{\partial \varphi} = 0, \quad (46)$$

We reformulate *equation (46)* into a new form as

$$\frac{\partial}{\partial r} (r^2 t(r) \tau_{r\varphi}) + r t(r) \frac{\partial \sigma_\varphi}{\partial \varphi} = 0. \quad (47)$$

Integration of *equation (47)* yields

$$\tau_{r\varphi}(r, \varphi) = -\frac{1}{r^2 t(r)} \int_0^r \rho t(\rho) \frac{\partial \sigma_\varphi}{\partial \varphi} d\rho, \quad b \leq r < c, \quad (48)$$

$$\tau_{r\varphi}(r, \varphi) = \frac{c^2 t_2 \tau_2(\varphi)}{r^2 t(\varphi)} - \frac{1}{r^2 t(r)} \int_0^r \rho t(\rho) \frac{\partial \sigma_\varphi}{\partial \varphi} d\rho, \quad c \leq r < a, \quad (49)$$

where

$$\tau_2(\varphi) = \lim_{\varepsilon \rightarrow 0} \tau_{r\varphi}(c - \varepsilon^2, \varphi). \quad (50)$$

The validity of *formula (49)* follows from the next *equation*

$$t_2 \tau_2(\varphi) = t_1 \lim_{\varepsilon \rightarrow 0} \tau_{r\varphi}(c + \varepsilon^2, \varphi). \quad (51)$$

The computation of the radial normal stress $\sigma_r = \sigma_r(r, \varphi)$ is based on *equation (45)*. From *equation (45)* we obtain

$$\sigma_r(r, \varphi) = \frac{1}{r t(r)} \int_b^r t(\rho) \left(\sigma_\varphi(\rho, \varphi) - \frac{\partial \tau_{r\varphi}}{\partial \varphi} \right) d\rho, \quad b \leq r < c, \quad (52)$$

$$\sigma_r(r, \varphi) = \frac{c t_2 \sigma_2}{r t(r)} + \frac{1}{r t(r)} \int_c^r t(\rho) \left(\sigma_\varphi(\rho, \varphi) - \frac{\partial \tau_{r\varphi}}{\partial \varphi} \right) d\rho, \quad c \leq r < a. \quad (53)$$

Here,

$$\sigma_2(\varphi) = \lim_{\varepsilon \rightarrow 0} \sigma_r(c - \varepsilon^2, \varphi) \quad (54)$$

and we use the continuity condition of radial normal stress resultant at $r = c$, which can be formulated as

$$t_2 \sigma_2(\varphi) = t_1 \lim_{\varepsilon \rightarrow 0} \sigma_r(c + \varepsilon^2, \varphi). \quad (55)$$

Solution of differential *equation*

$$\frac{d^2 U}{d\varphi^2} + U = K_1 \sinh(\Omega \varphi) + K_2 \cosh(\Omega \varphi) + \frac{MR}{E_0 A (R - r_3)} \quad (56)$$

for $U = U(\varphi)$ gives the expression of radial displacement

$$U(\varphi) = \frac{K_1}{1+\Omega^2} \sinh(\Omega\varphi) + \frac{K_2}{1+\Omega^2} \cosh(\Omega\varphi) + \frac{MR}{E_0 A (R-r_3)} + U_0(\varphi). \quad (57)$$

In equation (57) $U_0 = U_0(\varphi)$ is the general solution of the homogeneous differential equation

$$\frac{d^2 U_0}{d\varphi^2} + U_0 = 0 \quad (58)$$

which is represented as

$$U_0(\varphi) = K_3 \cos \varphi + K_4 \sin \varphi. \quad (59)$$

The values of the constants of integration K_3 and K_4 have no effect the stress, $U_0 = U_0(\varphi)$ describes a possible rigid body motion of the two-layer composite curved beam. For the case $k = \infty$ (perfect connection) the radial displacement, when the cross section at $\varphi = 0$ fixed, is determined by the next boundary conditions (Ecsedi and Dluhi, 2005)

$$U(0) = 0 \quad \text{and} \quad \left(\frac{dU}{d\varphi} \right)_{\varphi=0} = 0. \quad (60)$$

To compare the radial displacement of curved beam with inter-layer slip with perfect bonded two-layer curved beam we use to get K_3 and K_4 equation (60). A simple computation yields the result

$$K_3 = - \left(\frac{K_2}{1+\Omega^2} + \frac{MR}{E_0 A (R-r_3)} \right), \quad (61)$$

$$K_4 = - \frac{\Omega}{1+\Omega^2} K_1. \quad (62)$$

The computation of the slip function is based on the next equation

$$s(\varphi) = \frac{1}{kc^2 t} \frac{dM_1}{d\varphi} = c(\phi_1(\varphi) - \phi_2(\varphi)). \quad (63)$$

A detailed computation yields the result

$$s(\varphi) = \frac{A_1 E_1}{kc^2 t} \left(1 + \frac{r_1 R - r_2 E_0 A}{R r_2 - r_1 E_1 A_1} \right) \frac{dW}{d\varphi}. \quad (64)$$

5. Examples

5.1. Example 1

The cross section of the two-layer curved beam is shown in *figure 3*. The following data are used

$$a = 0.04 \text{ m}, \quad b = 0.02 \text{ m}, \quad c = 0.03 \text{ m}, \quad t = 0.005 \text{ m},$$

$$E_1 = 10 \times 10^{11} \text{ Pa}, \quad E_2 = 8 \times 10^{10} \text{ Pa}, \quad k = 50 \times 10^{10} \text{ N/m}^3,$$

$$\bar{M}_{11} = \bar{M}_{12} = 300 \text{ Nm}, \quad \bar{M}_{21} = \bar{M}_{22} = -300 \text{ Nm},$$

$$M = \bar{M}_{11} + \bar{M}_{21} = \bar{M}_{21} + \bar{M}_{22} = 0, \quad \alpha_1 = 0, \quad \alpha_2 = \pi.$$

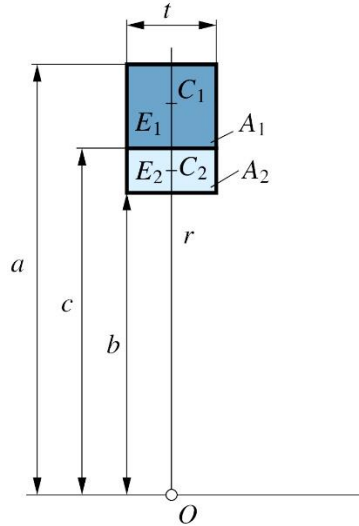


Figure 3. The cross section of curved composite beam

The graphs of $\sigma_\varphi = \sigma_\varphi(r, \varphi)$, $\sigma_r = \sigma_r(r, \varphi)$ and $\tau_{r\varphi} = \tau_{r\varphi}(r, \varphi)$ as a function of radial coordinate for cross sections given by polar angle $\varphi = 0$, $\varphi = \pi/6$, $\varphi = \pi/4$, and $\varphi = 3\pi/4$ are shown in figures. 4, 5 and 6. The graphs of radial displacement and slip function as a functions of polar angle φ are presented in figures 7 and 10.

The circumferential displacement and the cross-sectional rotation are shown in figures 8 and 9 as a function of polar angle φ .

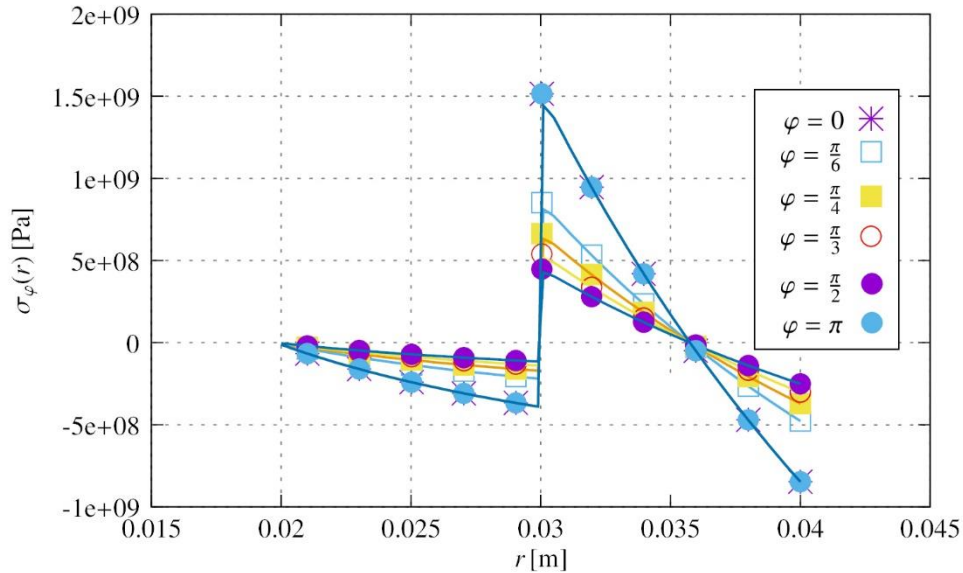


Figure 4. Plots of the circumferential normal stresses for example 1

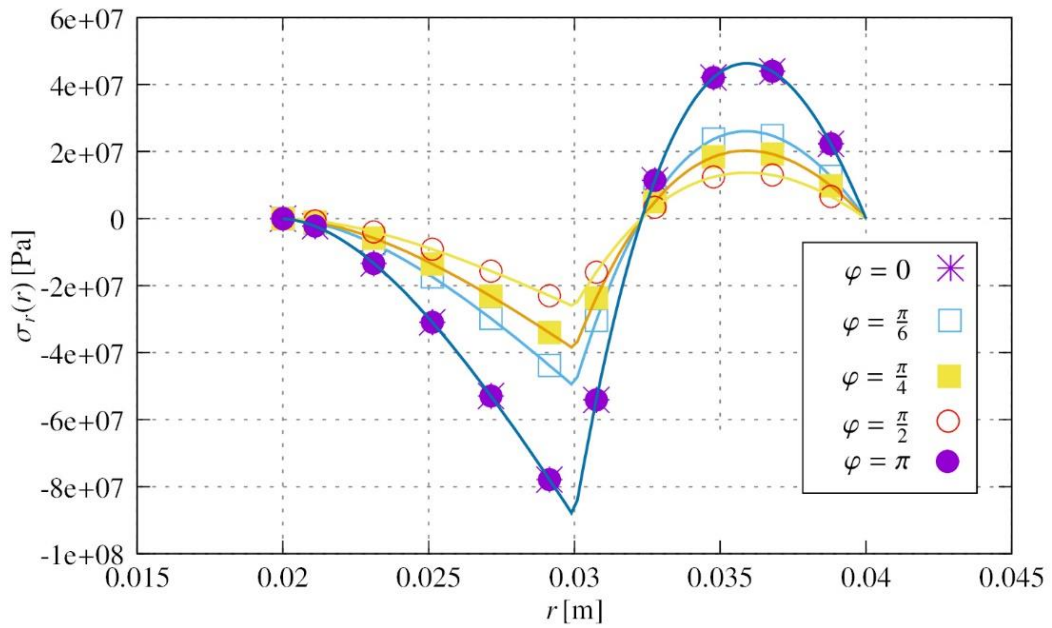


Figure 5. Plots of the radial normal stresses for example 1

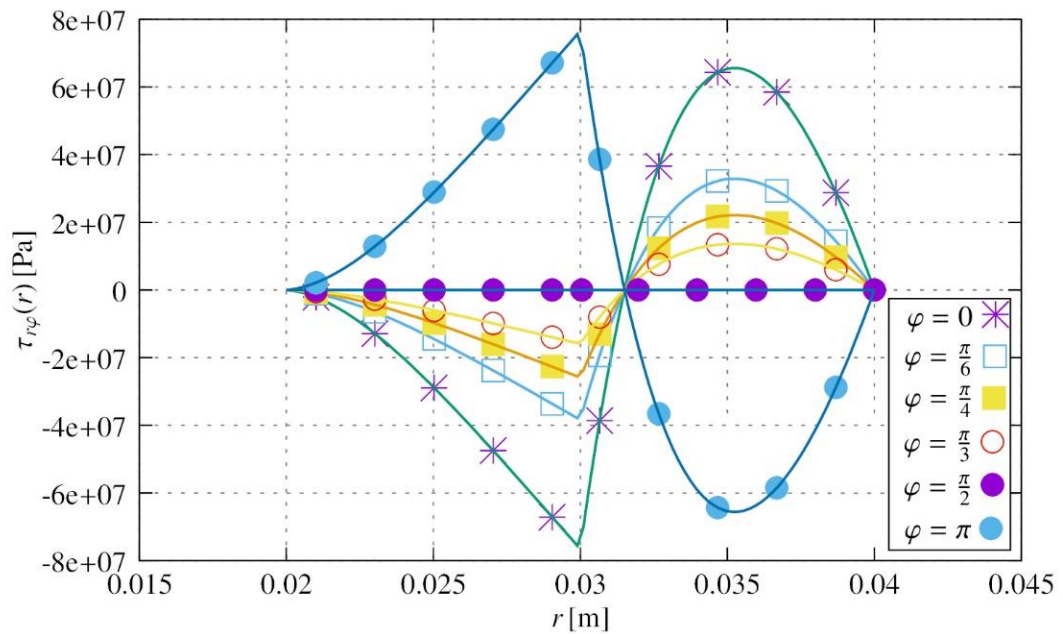


Figure 6. Plots of shearing stresses for example 1

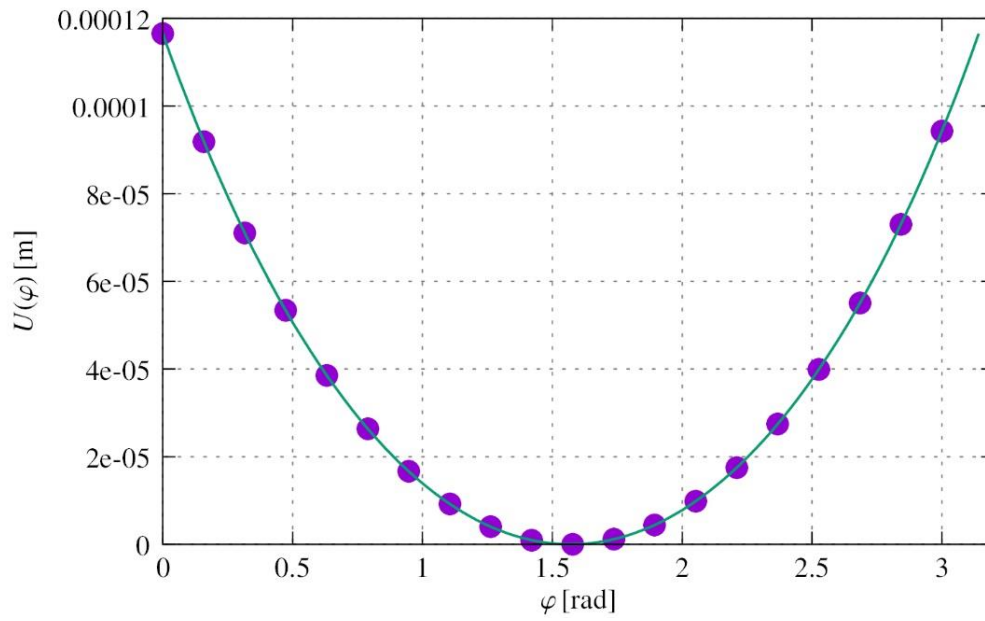


Figure 7. Plot of the radial displacement for example 1

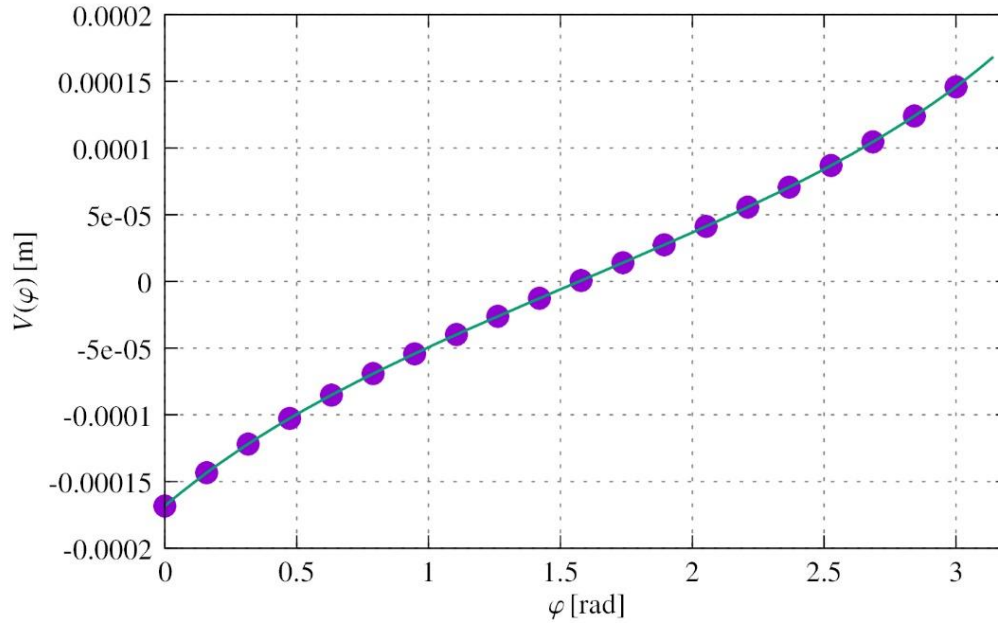


Figure 8. Plot of the displacement in circumferential direction for example 1

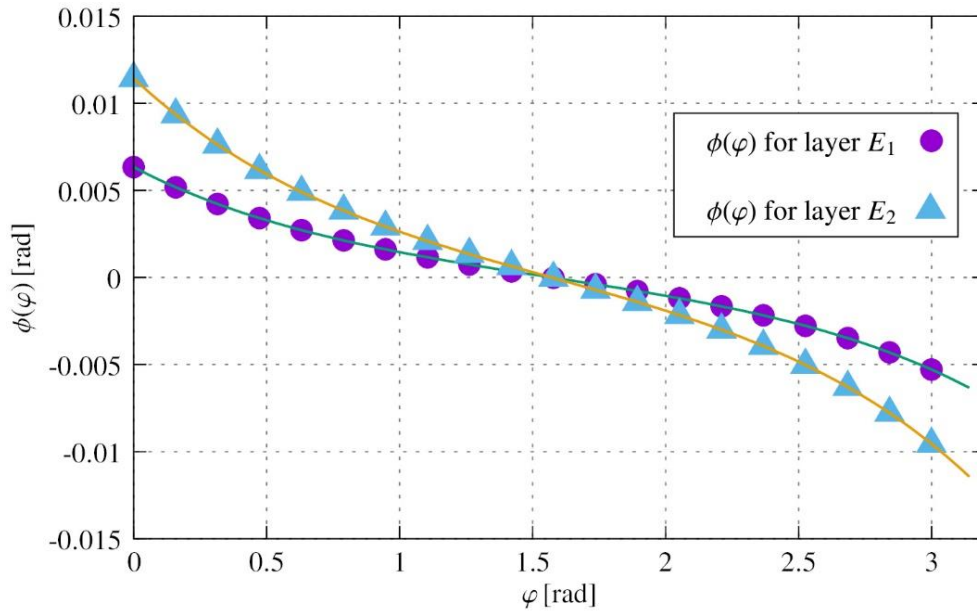


Figure 9. Plot of the cross-sectional rotation for example 1

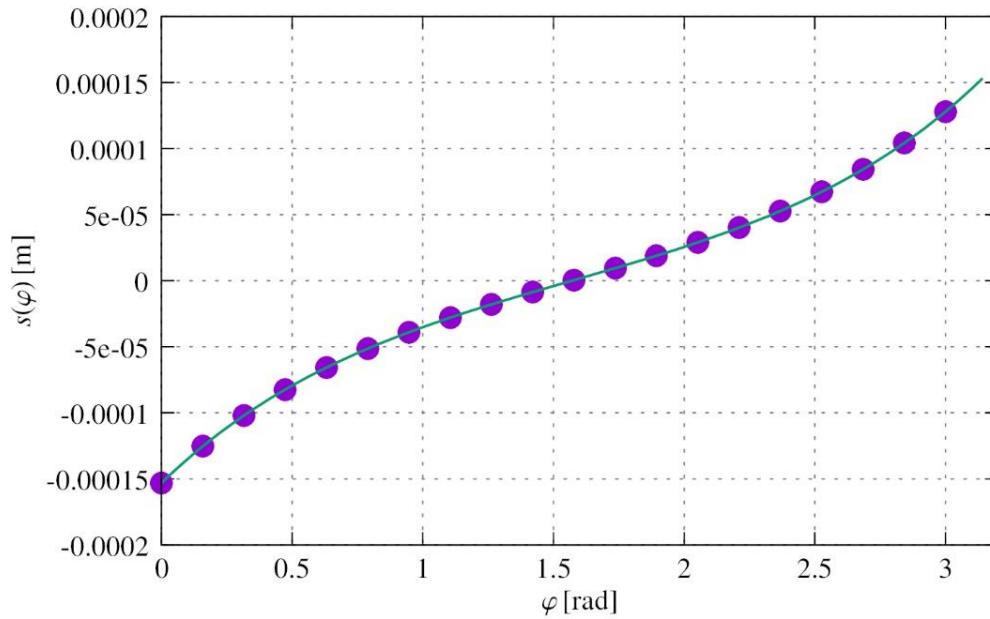


Figure 10. Plot of slip function for example 1

5.2. Example 2

The data of example 2 are the same as were used in example 1 except the applied end bending moments which as follows

$$\bar{M}_{11} = \bar{M}_{12} = 200 \text{ Nm}, \quad \bar{M}_{21} = \bar{M}_{22} = -200 \text{ Nm},$$

that is

$$M = \bar{M}_{11} + \bar{M}_{21} = \bar{M}_{21} + \bar{M}_{22} = 0.$$

The end loads at the cross section α_1 and α_2 are on equilibrium force system.

In figures 11, 12 and 13 the graphs of the stresses σ_φ , σ_r and $\tau_{r\varphi}$ are illustrated. Figure 14 shows the graphs of the functions $M_1 = M_1(\varphi)$ and $M_2 = M_2(\varphi)$.

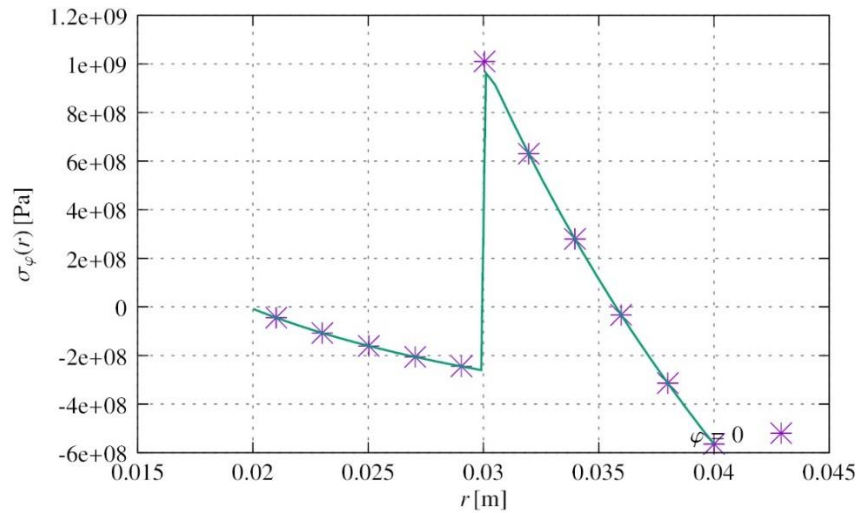


Figure 11. Plots of the circumferential normal stresses for $M = 0$ for example 2

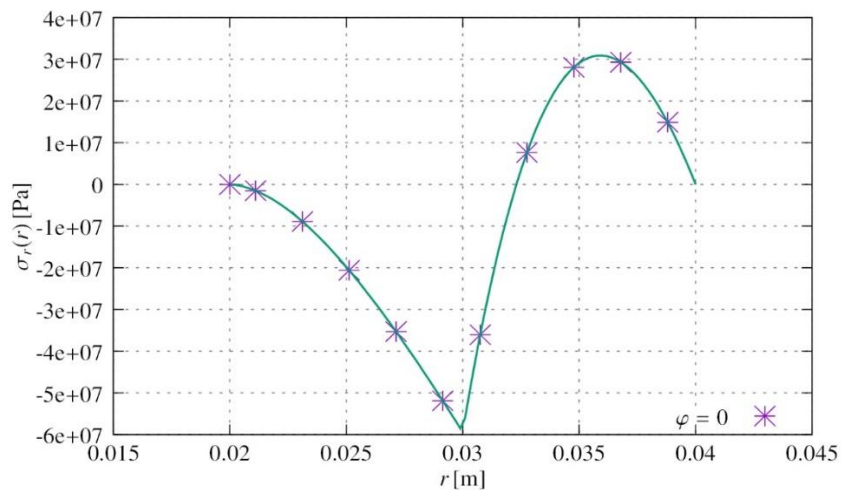


Figure 12. Plots of the radial normal stresses for $M = 0$ for example 2

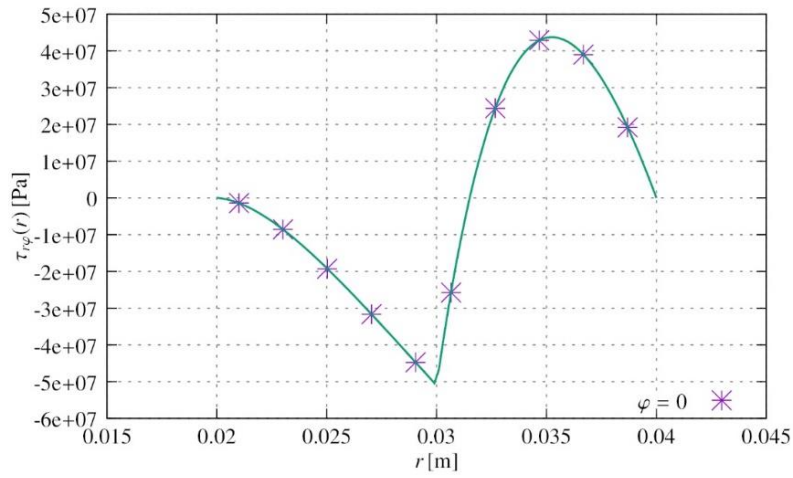


Figure 13. Plots of the shearing stress for $M = 0$ for example 2

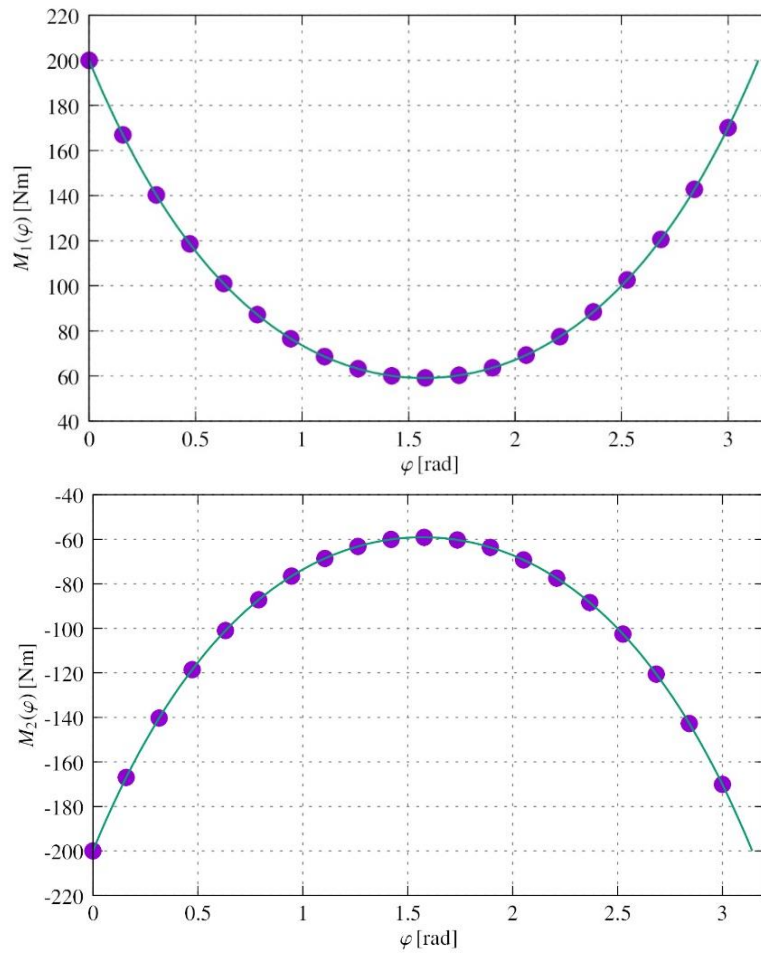


Figure 14. Plots of the functions $M_1 = M_1(\varphi)$ and $M_2 = M_2(\varphi)$ for example 2

6. Summary

The presented investigation gives an example of the pure bending of two-layered curved beams made of different elastic isotropic material. We work on the extension of this analysis to elastic anisotropic material.

We are planning a detailed examination of the pure bending problem for mixed type boundary conditions, when for example, the bending moment is prescribed only the end cross sections of upper layer. The end cross sections of lower layer have given cross-sectional rotations.

In this paper two-layer curved beam with deformable shear connection is analysed. The curved composite beam is subjected to bending moments applied them at its end cross section. A model developed to describe the static behaviour of the two-layer curved beam which is based on the Euler-Bernoulli beam theory. It is shown that under the action of pure bending moment in the composite curved beam with imperfect shear connection the shearing stresses appear too.

References

- [1] Granholm, H. (1949). On Composite Beams and Columns with Special Regard to Nailed Timber Structures. Trans., No. 88. Chalmers University of Technology, Goeteborg, Sweden.
- [2] Pleskov, P. F. (1952). Theoretical Studies of Composite Wood Structures. Soviet Union, Moscow.
- [3] Stüssi, F. (1949). Zusammengesetzte vollwandträger. Assoc. Bridge Struct. Eng. (IABSE) 8, 249-269.
- [4] Newmark, N. M., Siess, C. P., Viest, I. M. (1949). Test and analysis of composite beam with incomplete interaction. Proc. Soc. Expl. Stress Anal., pp. 975-992.
- [5] Girhammer, U. A., Gopu, V. K. A. (1993). Composite beam-columns with interlayer-slip-exact analysis. ASCE J Struct. Eng., 119 (4), pp. 1265-1282. [https://doi.org/10.1061/\(ASCE\)0733-9445\(1993\)119:4\(1265\)](https://doi.org/10.1061/(ASCE)0733-9445(1993)119:4(1265))
- [6] Planic, I., Schnabl, S., Saye, M., Lopatic, J., Cas, B. (2008). Numerical and experimental analysis of timber composite beams with interlayer slip. Engineering and Structures, 30, pp. 2959-2969. <https://doi.org/10.1016/j.engstruct.2008.03.007>
- [7] Girhammar, U. A., Pan, D. (2007). Exact analysis of partially composite beams and beam-columns. International Journal of Mechanical Sciences, 49 (2), pp. 239-255. <https://doi.org/10.1016/j.ijmecsci.2006.07.005>
- [8] Goodman, J. R., Popov, E. P. (1968). Layered beam systems with inter-layer slip. Journal of Struct. Division-ASCE Science, 94 (11), pp. 2537-2547. <https://doi.org/10.1061/JSDEAG.0002116>
- [9] Goodman, J. R., Popov, E. P. (1969). Layered wood systems with inter-layer slip. Wood Science, 1 (3), pp. 148-158.
- [10] Ecsedi, I., Lengyel, A. J. (2015). Curved composite beam with interlayer slip loaded by radial load. Curved and Layered Structures, 2 (1), pp. 50-58. <https://doi.org/10.1515/cls-2015-0004>
- [11] Ecsedi, I., Lengyel, A. J. (2015). Energy methods for curved composite beams with partial shear

- interaction. *Curved and Layered Structures*, 2 (1), pp. 351-361. <https://doi.org/10.1515/cls-2015-0020>
- [12] Ecsedi, I., Dluhi, K. (2005). A linear model for static and dynamic analysis of nonhomogeneous curved beams. *Applied Mathematical Modelling*, 29, pp. 1211-1231. <https://doi.org/10.1016/j.apm.2005.03.006>
- [13] Sokolnikoff, I. S. (1956). *Mathematical Theory of Elasticity*. McGraw-Hill, New York.